Hindawi
Advances in Materials Science and Engineering
Volume 2019, Article ID 1670478, 7 pages
https://doi.org/10.1155/2019/1670478

Research Article

Flexural Behavior of Basalt Fiber Reinforced Polymer Tube Confined Coconut Fiber Reinforced Concrete

Yang Lv ,[1,2] Xueqian Wu,[1] Mengran Gao,[1] Jiaxin Chen,[2] Yuhao Zhu,[1] Quanxi Cheng,[1] and Yu Chen [3]

[1]*Tianjin Key Laboratory of Civil Structure Protection and Reinforcement, Tianjin Chengjian University, Tianjin 300384, China*
[2]*Department of Civil and Environmental Engineering, The University of Auckland, Private Bag 92019, Victoria Street West, Auckland 1142, New Zealand*
[3]*Airport College, Civil Aviation University of China, Tianjin 300300, China*

Correspondence should be addressed to Yu Chen; tjucy@tju.edu.cn

Received 30 November 2018; Accepted 8 January 2019; Published 3 February 2019

Academic Editor: Carlo Santulli

Copyright © 2019 Yang Lv et al. This is an open access article distributed under the Creative Commons Attribution License, which permits unrestricted use, distribution, and reproduction in any medium, provided the original work is properly cited.

Basalt fiber has arisen new perspectives due to the potential low cost and excellent mechanical performance, together with the use of environmental friendly coir can be beneficial to the development of sustainable construction. In this study, a new composite structure called basalt fiber reinforced polymer (BFRP) tube encased coconut fiber reinforced concrete (CFRC) is developed. The 28-day compression strength of the plain concrete is about 15 MPa, which represents the low-strength poor-quality concrete widely existing in many old buildings and developing countries. Three types of BFRP tubes, i.e., 2-layer, 4-layer, and 6-layer, with the inner diameter of 100 mm and a length of 520 mm, were prepared. The plain concrete (PC) and CFRC were poured and cured in these tubes to fabricated BFRP tube confined long cylindrical beams. Three PC cylindrical beams and 3 CFRC cylindrical beams were prepared to be the control group. The four-point bending tests of these specimens were carried out to investigate the enhancement due to the BFRP tube and coir reinforcement. The load-carrying capacity, force-displacement relationship, failure mode, and the cracking moment were analyzed. Results show that both BFRP tube confined plain concrete (PC) and BFRP tube confined CFRC have excellent flexural strength and ductility, and the inclusion of the coir can further enhance the ductility of the concrete.

1. Introduction

In the last years, an increasing interest in environmental issues has promoted the employment of natural fibers in polymer reinforcing. Natural vegetable fibers such as flax fiber, bamboo fiber, abaca fiber, sisal fiber, coir, and cotton fiber are most popularly studied [1–3]. Considering the economy, mechanical properties, and sustainability, coir has gained popularity among the most natural vegetable fibers. Every year, a large amount of coir shell garbage is generated around the world. Coir is an agricultural waste product obtained in the processing of coir oil. Adding a certain amount of coir into concrete can improve the performance of the concrete and make full use of many agricultural waste products [4]. Many studies have shown that coir has a positive effect on increasing the compressive strength, flexural strength, shear strength, dynamic properties, and ductility of concrete [5–7]. However, the properties of the coconut fiber reinforced concrete (CFRC) are significantly influenced by the length and content of coir. Research studies [6] reveal that CFRC with 50 mm long fibers and less than 5% fiber content has an obvious improvement on the concrete properties.

Adding natural fibers into concrete is one of the ways to improve the performance of concrete. Fiber reinforced polymer confined concrete is another efficient way. In 1982, Park et al. proposed that the strength of traditional reinforced concrete must be strengthened in addition to the consideration of earthquake action [8]. At the same time, Macdonald and Calder had begun to use steel tube to confine concrete, and after that, more and more researchers began to study confined concrete [9–14]. From the perspective of sustainable development, fiber reinforced polymer (FRP), such as glass fiber, carbon fiber, flax fiber, and basalt fiber, has become the major research direction. The research studies show that this kind of confined concrete has the characteristics of high strength, high stiffness, good ductility, and strong stability. Based on this, a new type of structure, FRP tube confined fiber reinforced concrete, has been proposed. Yan and Chouw had studied flax fiber-confined coir concrete (FFRP-CFRC) and found that the new structure has the advantages of two different fiber materials and can significantly improve the concrete performance [15, 16]. Chen and Chouw studied the flexural properties of the flax fiber double-tube confined coir reinforced concrete (DFFRP-CFRC), and their research revealed that the flexural stiffness, cracking strength, and the ultimate load-bearing capacity of DFFRP-CFRC beam could be improved due to an additional longitudinal reinforcement provided by the inner FFRP tube [17].

Recently, basalt fiber gains popularity in the field of the construction engineering. Compared with glass fiber reinforced polymer (GFRP) and carbon fiber reinforced polymer (CFRP), basalt fiber has superior characteristics such as high strength to weight ratio, excellent ductility and durability, high thermal resistance, good corrosion resistance, and cost-effective [18, 19]. Wu et al. studied the seismic behavior of concrete columns strengthened by basalt fiber reinforced polymer (BFRP) and coir reinforced concrete (CFRP), and they found that the reinforcement of BFRP can significantly improve the seismic performance of the concrete circular columns [20]. Considering the mechanical properties and cost-effectiveness, basalt fiber is a good alternative to carbon fiber and glass fiber in the future [21].

In this study, 9 BFRP tubes confined PC cylindrical beams, 9 BFRP tubes confined CFRC cylindrical beams, and 3 PC and 3 CFRC cylindrical beams as the control group were prepared. The four-point bending tests of these specimens were carried out to investigate the enhancement due to the BFRP tube and coir reinforcement. Results show that both BFRP tube confined PC and BFRP tube confined CFRC have excellent flexural strength and ductility. The inclusion of the coir can further enhance the ductility of the concrete.

2. Experiments

2.1. Test Specimens and Materials. Commercial bidirectional woven basalt fabric (300 g/m^2) was used for this study. The fabric has a plain woven structure with a count of 5.5 threads/cm in both warp and weft directions. The epoxy resin and hardener used in this experiment were RIM035C and RIMH037 provided by Hoxion. The mix ratio is 100 : 18 for the epoxy resin and hardener. BFRP tubes were wrapped around an acrylic tube mould using a hand lay-up process. The outside diameter of the mould is 100 mm. After 24 hours curing in room temperature, the tubes were demoulded and were put into an oven for 8 hours with a constant temperature of 80°C to increase the hardening. The tubes contain two-layer, four-layer, and six-layer arrangements, with each layer arrangement built six tubes. Figure 1 gives the BFRP tubes waiting for concrete pouring. Nine coupons were fabricated and cured in the same condition with the BFRP tubes, and the coupons were tested on a universal testing machine according to ASTM D3039 [22]. The mechanical properties of basalt fiber composites are listed in Table 1. Figure 2 shows the stress-strain relationship of BFRP coupons of 2-layer, 4-layer, and 6-layer. The modulus of the BFRP is between 13.0 and 15.0 GPa. Coir mechanical properties can be found in the study by Yan [23].

Figure 1: BFRP tubes for concrete pouring.

The coconut fiber was supplied by a factory, which they collected directly from the farmers. Before we add the messy fiber into the concrete, it was cut to lengths between 30 and 70 mm, and the mean value is about 50 mm. This is reasonable in practical use. The coconut fiber content was 1% of the cement mass. Two batches of concrete without and with coir were prepared. Both batches were designed as PC with a 28-day compression strength of 15 MPa to represent the low-strength concrete. In the second batch, coconut fiber was added. The concrete mix ratio [24] by mass was 1 : 0.58 : 3.72 : 2.37 : 0.00245 for cement: water: gravel: sand: water reducer, respectively. The cement used was 32.5 normal Portland cement. The gravel has a maximum size of 25 mm. The natural sand was used as fine aggregate with a fineness modulus of 2.75. All the specimens have an inner diameter of 100 mm and a length of 520 mm. The matrix of the specimens prepared for this study consists of 24 cylindrical specimens and is given in Table 2. To facilitate the pouring and curing of the concrete, the BFRP tubes were fixed on a wooden base by a hot melt adhesive.

2.2. Instrumentation and Test Setup. To carry out the four-point bending test [25], three strain gauges were mounted in the middle of the specimen aligned along the axial direction and three strain gauges were mounted perpendicularly to the former three strain gauges, i.e., aligned along the hoop direction. One linear variable displacement transducer (LVDT) was placed below the middle of the specimen to measure the deflection of the specimen, and two LVDTs were placed between the loading steel plates. The layout of the four-point bending test is shown in Figure 3. The test data of the load cell, strain gauges, and LVDTs were taken using a data acquisition system and were stored in a computer.

Table 1: Mechanical properties of basalt fiber composites.

No. of layers	Composite thickness (mm)	Tensile stress (MPa)	Tensile modulus (GPa)	Tensile fracture strain (%)	Volume fraction (%)	Density (g/cm^3)
2	1.10	411.00	13.14	3.24	59.29%	1.867
4	1.75	453.29	14.25	4.38	59.71%	1.872
6	2.60	497.19	14.97	4.8	62.21%	1.818

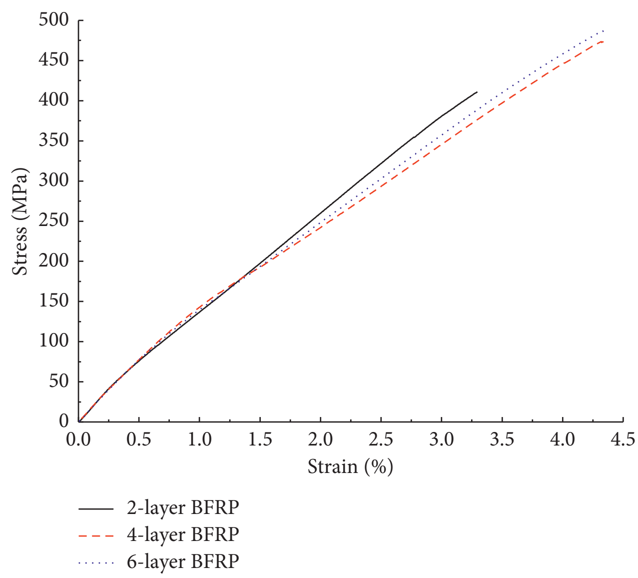

Figure 2: Stress-strain relationship of BFRP.

Table 2: Test matrix of specimens with a height of 520 mm and an inner diameter of 100 mm.

Specimens	No. of BFRF layers	Tube thickness (mm)	Mass (kg)	28-day compressive strength (MPa)
PC	—	0	9.93	18.0
CFRC	—	0	9.91	18.81
2L-BFRP-RC	2	1.06	10.13	23.1
4L-BFRP-RC	4	1.57	10.33	32.3
6L-BFRP-RC	6	2.29	10.37	38.5
2L-BFRP-CFRC	2	1.04	10.05	28.2
4L-BFRP-CFRC	4	1.58	10.31	31.4
6L-BFRP-CFRC	6	2.25	10.46	41.1

3. Results and Discussions

3.1. Load-Displacement Relationship. The peak load and maximum deflection of the long cylindrical specimens are summarized in Table 3. The load-displacement curves for BFRP-PC and BFRP-CFRC are provided in Figure 4. From Figure 4, it is clear to see that the load-carrying capacity and deformation capacity of the BFRP tube confined concrete significantly improved compared to the unconfined concrete specimens. The load-carrying capacity of the 2-layer,

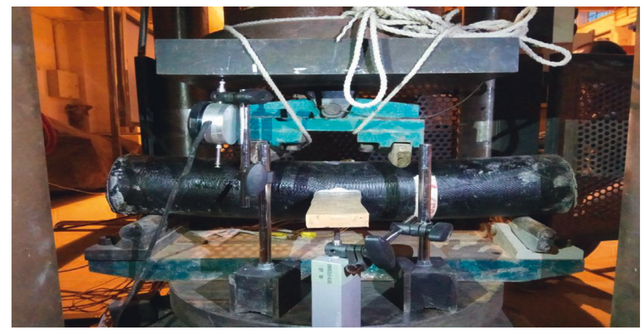

Figure 3: Setup of the four-point bending test.

4-layer, and 6-layer BFRP tube confined PC cylindrical specimens increased about 538.63%, 1082.39%, and 1572.15% comparing to the PC specimens, respectively. The corresponding deformation capacity increased about 949.51%, 1106.33%, and 1277.30% comparing to the PC specimens. For the BFRP confined CFRC specimens, the load-carrying capacity for 2-layer, 4-layer, and 6-layer tubes increased about 739.42%, 1481.54%, and 2148.90% comparing to the CFRC specimens, respectively. The corresponding deformation capacity increased about 875.17%, 1117.69%, and 1293.54% comparing to the CFRC specimens. The stiffness of the specimen has been significantly improved due to the confinement of the BFRP tube. The load-carrying capacity and the deformation capacity increase with the thickness of the BFRP tube, the load-carrying capacity and deformation capacity of the 4-layer BFRP tube confined PC beam increased about 100.98% and 16.53% comparing to the 2-layer BFRP tube confined PC, respectively, and the load-carrying capacity and deformation capacity of the 6-layer BFRP tube confined PC beam increased about 45.25% (from 47.03 kN to 68.31 kN) and 15.46% (from 28.27 mm to 32.64 mm) comparing to the 4-layer BFRP tube confined PC, respectively. For the BFRP tube confined CFRC beams, the increases of load-carrying capacity and deformation capacity between 4-layer and 2-layer specimens are 100.33% and 24.87%, respectively. The increases of load-carrying capacity and deformation capacity between 6-layer and 4-layer specimens are 45.05% and 16.79%, respectively. It was found that there was a slight enhancement comparing BFRP-CFRC to BFRP-PC. From Table 3, it is also shown that the inclusion of coir will slightly increase the load-carrying capacity and can significantly increase the deformation capacity.

It should be noted that the force-displacement curves were not smooth, several sudden drops were experienced during the loading process; the reason is that the slippage between the concrete core and BFRP tube happened

Table 3: Average test results of long cylindrical specimens under flexure.

Specimens	Peak load (kN)	Increase due to the tube compared to PC (%)	Increase due to coir compared to BFRP-PC (%)	Maximum deflection (mm)	Deflection increase due to the tube compared to PC (%)	Deflection increase due to coir compared to BFRP-PC (%)
PC	4.35	—	—	2.56	—	—
2L-BFRP-PC	23.40	538.63	—	24.26	949.51	—
4L-BFRP-PC	47.03	1082.39	—	28.27	1106.33	—
6L-BFRP-PC	68.31	1572.15	—	32.64	1277.30	—
CFRC	3.99	—	−8.28	2.94	—	14.84
2L-BFRP-CFRC	24.70	739.42	5.56	28.67	875.17	18.18
4L-BFRP-CFRC	49.48	1481.54	5.21	35.80	1117.69	26.65
6L-BFRP-CFRC	71.77	2148.90	5.07	40.97	1293.54	25.54

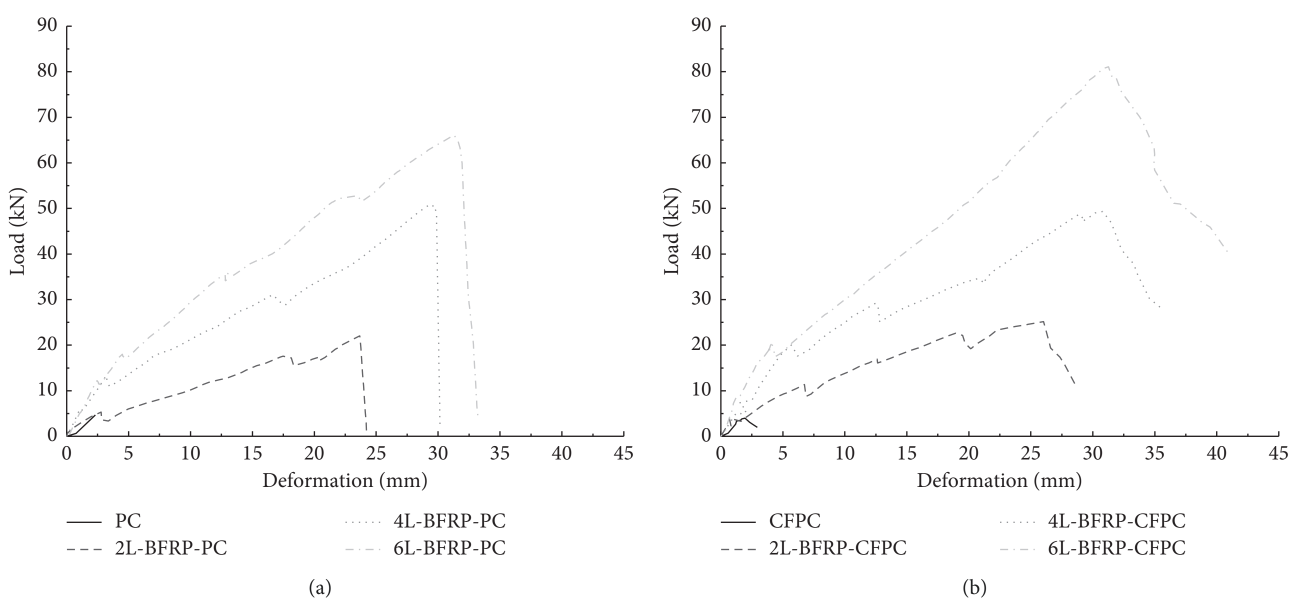

Figure 4: Load-displacement relationship. (a) PC and BFRP-PCs. (b) CFRC and BFRP-CFRCs.

constantly. The BFRP tube confined PC beams undergo a brittle failure after the peak load, while the BFRP tube confined CFRC beams show excellent deformation capacity even exceeding the peak load; this is mainly due to the bridging effect of the coir in concrete.

3.2. Failure Modes. The failure modes of BFRP tube confined PC and CFRC specimens and the PC and CFRC cores after the tests are shown in Figure 5. For the PC specimens without BFRP tube confinement, a sudden fracture was observed after the peak load for all specimens, and the load-carrying capacity and deformation capacity are extremely small, which cannot be used without reinforcement. For the CFRC specimens, the coir enhanced the deformation capacity due to the bridging effect, but there is little load-carrying capacity enhancement. All the BFRP tube confined PC and CFRC specimens failed due to the sudden fracture of the BFRP tubes. At the beginning of the bending test, the load decreased because of the cracking of the core beam. At the same time, the confinement of the BFRP tube is activated. From the bending tests carried out in this study, there are three types of failure modes. One is the bending failure at the constant moment region such as 2-layer and 4-layer BFRP tube confined PC and CFRC in Figures 5(a)–5(d). This failure mode is due to the tensile fracture of the BFRP. It experienced excellent load-carrying and deformation performance. The second failure mode is the bend-shear combination failure at the bend-shear region like the specimen 6L-BFRP-PC in Figure 5(e). The BFRP tube was torn gradually during the loading process. The reason for this failure mode is the compression strength of the core concrete is very low, and the BFRP tube significantly enhanced the ultimate bending moment; however, the shear

(a) (b) (c) (d) (e) (f) (g) (h)

Figure 5: Failure modes. (a) 2L-BFRP-PC. (b) 2L-BFRP-CFRC. (c) 4L-BFRP-PC. (d) 4L-BFRP-CFRC. (e) 6L-BFRP-PC. (f) 6L-BFRP-CFRC. (g) PC core. (h) CFRC core.

capacity has a little increase; therefore, this failure mode is controlled by the shear capacity of the specimen. The third failure mode is due to the local compression failure of the concrete at the supporting points like the specimen 6L-BFRP-CFRC in Figure 5(f). This failure mode is somehow similar to the second failure mode, the reason is that the BFRP tube increased the ultimate bending moment; however, the BFRP tube was cut off by the small cylindrical supports and followed by the crush of the low-strength concrete at the supporting points. From the failure modes of the 2-layer, 4-layer, and 6-layer BFRP tubes confined PC and CFRC beams, it can be inferred that there is a balance among these failure modes that the specimen has identical bend-carrying capacity and shear-carrying capacity. All the parameters connected with the bend-carrying capacity and shear capacity will influence the failure mode of the beams, such as the thickness of the BFRP tube, the strength of the core concrete, the shear span of the beam, and the types of the supporting. The inclusion of coir has little influence on the failure mode of the BFRP tube confined concrete except a little larger load-carrying capacity and deformation capacity. From Figures 5(g) and 5(h), it is shown that the core of BFRP tube confined PC beam was fractured into three parts at the end of the bending test. The locations of the fracture occurred near the two loading points, and an apparent wide crack went through the midpoint. The failure mode of the CFRC core was similar to that of the PC core, but there are still some connections between the nearby two parts of concrete by the coir.

3.3. Cracking Moment. As mentioned in the previous section, the load-displacement curves of the BFRP tube confined PC and CFRC beams have a decrease at the beginning of the test. This phenomenon is due to the cracking of the concrete core. Assuming that the BFRP tube and the concrete core are elastic, the cracking moment of BFRP-PC and BFRP-CFRC can be predicted according to the following equation:

$$M_{\mathrm{cr}} = \frac{f_{\mathrm{r}} I_{\mathrm{g}}}{y_{\mathrm{t}}}, \tag{1}$$

where f_{r} is the cracking strength of the concrete, I_{g} is the moment of inertia of the gross section, and y_{t} is the distance from the gravity center of the beam to the extreme tension fiber. The cross-sectional moment of inertia I_{g} can be calculated using the following equation [26]:

$$I_g = I_{core} + \gamma I_{tube},$$
$$I_{core} = \frac{\pi D^4}{64}, \quad (2)$$
$$I_{tube} = \frac{\pi\left[(D+2t)^4 - D^4\right]}{64},$$

where γ is the ratio of the modulus of elasticity of the BFRP tube to the modulus of elasticity of the concrete $\gamma = (E_{tube}/E_{core})$, Young's modulus of concrete [27] can be determined using $E_{core} = 5000\sqrt{f'_{co}}$, and Young's modulus of the BFRP tube E_{tube} is given in Table 1. D is the inner diameter of the tube and t is the thickness of the tube.

The cracking strength of concrete according to ACI Building Code 318-08 is

$$f_{cr} = k\sqrt{f'_{co}}, \quad (3)$$

where $k = 0.6$ in ACI Building Code 318-08 [28], and $k = 0.4$ and 1.0 in the Canadian Highway Bridge Design Code CSA CAN/CSA S6-06 Bridge code [27] by Fam and Rizkalla [26], respectively. The cracking moment measured by the test and the predicted cracking moment using the formulas are listed in Table 4; *Ratio* is the ratio of the experimental cracking moment to the predicted cracking moment.

Yan and Chouw [29] had studied the cracking moment of flax fiber reinforced polymer tube confined concrete and coir reinforced concrete (FFRP-PC and FFRP-CFRC), their research revealed that the experimental cracking moment of FFRP-PC and FFRP-CFRC was larger than the conventional steel reinforced concrete beams but were smaller than the prediction proposed by Fam [30], similar conclusions can be obtained from Table 4, and the cracking moments of both BFRP-PC and BFRP-CFRC are much larger than that of the conventional steel reinforced concrete beams. However, it should be noticed that the experimental cracking moments of BFRP-PC and BFRP-CFRC were larger than the GFRP tube confined concrete considered by Fam [30]. The main reason is due to the differences in Young's modulus of FFRP, GFRP, and BFRP composites, in which Young's modulus of FFRP composites [31] is the smallest and BFRP is the highest.

Table 4: Experimental and predicted cracking moments of BFRP-PC and BFRP-CFRC.

Specimens		Test	ACI 318-08	CAN/CSA S6-06	Fam and Rizkalla
2L-BFRP-PC	M_{cr} (N·m)	501.38	279.49	186.32	465.81
	Ratio	—	1.79	2.69	1.08
4L-BFRP-PC	M_{cr} (N·m)	526.50	289.12	192.74	481.86
	Ratio	—	1.76	2.64	1.06
6L-BFRP-PC	M_{cr} (N·m)	557.25	274.73	183.87	458.61
	Ratio	—	2.03	3.03	1.22
2L-BFRP-CFRC	M_{cr} (N·m)	552.00	299.03	199.35	498.38
	Ratio	—	1.91	2.86	1.15
4L-BFRP-CFRC	M_{cr} (N·m)	526.88	309.15	206.10	515.25
	Ratio	—	1.70	2.56	1.02
6L-BFRP-CFRC	M_{cr} (N·m)	585.00	282.60	186.39	466.52
	Ratio	—	2.07	3.14	1.25

4. Conclusions

The flexural behavior of BFRP tube confined CFRC beams were studied by the four-point bending test in this paper. Based on the test results of the force-displacement relationship, failure modes, and cracking moments, the following conclusions can be derived:

(1) BFRP tube can significantly improve the load-carrying capacity and deformation capacity of the composite beams.

(2) The inclusion of coir can slightly enhance the load-carrying capacity and significantly increase the deformation capacity of the beams.

(3) Compared with the conventional steel reinforced concrete beams, FFRP tube confined concrete beams, and GFRP tube confined concrete beams, the cracking moment of BFRP tube confined concrete beams is the largest because of highest Young's modulus of BFRP composites.

(4) The model proposed by Fam can precisely predict the cracking moment of the BFRP tube confined PC and CFRC beams; however, the models in ACI 318-08 and CAN/CSA S6-06 cannot predict the cracking moment.

Data Availability

The authors confirm that the data used to support the findings of this study are included within the article. If needed, the original data can be provided on request.

Conflicts of Interest

The authors declare that there are no conflicts of interest regarding the publication of this paper.

Acknowledgments

The authors gratefully acknowledge the partial support of this research by the National Key Research and Development Program of China under grant no. 2016YFC0701100, the National Natural Science Foundation of China under grant nos. 51508373, 51808380, and 51808270, and the Tianjin Basic Research Program under grant nos. 16JCZDJC38900 and 17JCTPJC51300. The authors would also like to thank the China Scholarship Council for supporting a one-year research stay of the first author at the University of Auckland.

References

[1] V. Agopyan Jr., H. Savastano, V. M. John, and M. A. Cincotto, "Developments on vegetable fibre-cement based materials in São Paulo, Brazil: an overview," *Cement and Concrete Composites*, vol. 27, no. 5, pp. 527–536, 2005.

[2] G. Khosrow, "Bamboo as reinforcement in structural concrete elements," *Cement and Concrete Composites*, vol. 27, no. 6, pp. 637–649, 2005.

[3] Y. Li, Y.-W. Mai, and L. Ye, "Sisal fibre and its composites: a review of recent developments," *Composites Science and Technology*, vol. 60, no. 11, pp. 2037–2055, 2000.

[4] N. M. S. Hasan, H. R. Sobuz, M. S. Sayed, and S. M. Islam, "The use of coconut fiber in the production of structural lightweight concrete," *Journal of Applied Science*, vol. 12, no. 9, pp. 831–839, 2012.

[5] P. Baruah and S. Talukdar, "A comparative study of compressive, flexural, tensile and shear strength of concrete with fibres of different origins," *Indian Concrete Journal*, vol. 81, pp. 17–24, 2007.

[6] M. Ali, A. Liu, H. Sou, and N. Chouw, "Mechanical and dynamic properties of coconut fibre reinforced concrete," *Construction and Building Materials*, vol. 30, no. 8, pp. 814–825, 2012.

[7] C. Asasutjarit, S. Charoenvai, J. Hirunlabh, and J. Khedari, "Materials and mechanical properties of pretreated coir-based green composites," *Composites Part B: Engineering*, vol. 40, no. 7, pp. 633–637, 2009.

[8] R. Park, M. J. N. Priestley, and W. D. Gill, "Ductility of square-confined concrete columns," *Journal of the Structural Division*, vol. 108, no. 4, pp. 929–950, 1982.

[9] M. D. Macdonald and A. J. J. Calder, "Bonded steel plating for strengthening concrete structures," *International Journal of Adhesion and Adhesives*, vol. 2, no. 2, pp. 119–127, 1982.

[10] L.-H. Han, G.-H. Yao, Z.-B. Chen, and Q. Yu, "Experimental behaviours of steel tube confined concrete (STCC) columns," *Steel and Composite Structures*, vol. 5, no. 6, pp. 459–484, 2005.

[11] E. Ellobody, B. Young, and D. Lam, "Behaviour of normal and high strength concrete-filled compact steel tube circular stub columns," *Journal of Constructional Steel Research*, vol. 62, no. 7, pp. 706–715, 2006.

[12] T. Yu, Y. L. Wong, J. G. Teng, S. L. Dong, and E. S. Lam, "Flexural behavior of hybrid FRP-concrete-steel double-skin tubular members," *Journal of Composites for Construction*, vol. 10, no. 5, pp. 443–452, 2006.

[13] P. Kushwaha and R. Kumar, "Enhanced mechanical strength of BFRP composite using modified bamboos," *Journal of Reinforced Plastics and Composites*, vol. 28, no. 23, pp. 2851–2859, 2008.

[14] T. Sen and H. N. Jagannatha Reddy, "Strengthening of RC beams in flexure using natural jute fibre textile reinforced composite system and its comparative study with CFRP and GFRP strengthening systems," *International Journal of Sustainable Built Environment*, vol. 2, no. 1, pp. 41–55, 2013.

[15] L. Yan and N. Chouw, "Experimental study of flax FRP tube encased coir fibre reinforced concrete composite column," *Construction and Building Materials*, vol. 40, no. 7, pp. 1118–1127, 2013.

[16] L. Yan and N. Chouw, "Dynamic and static properties of flax fibre reinforced polymer tube confined coir fibre reinforced concrete," *Journal of Composite Materials*, vol. 48, no. 13, pp. 1595–1610, 2013.

[17] J. Chen and N. Chouw, "Nonlinear flexural behaviour of flax FRP double tube confined coconut fibre reinforced concrete," *Materials & Design*, vol. 93, pp. 247–254, 2016.

[18] J. Sim, C. Park, and D. Y. Moon, "Characteristics of basalt fiber as a strengthening material for concrete structures," *Composites Part B: Engineering*, vol. 36, no. 6-7, pp. 504–512, 2005.

[19] V. Lopresto, C. Leone, and I. De Iorio, "Mechanical characterisation of basalt fibre reinforced plastic," *Composites Part B: Engineering*, vol. 42, no. 4, pp. 717–723, 2011.

[20] G. Wu, D. Gu, and J. Jiang, "Comparative study on seismic performance of circular concrete columns strengthened with BFRP and CFRP composites," *Industrial Construction*, vol. 37, no. 6, pp. 19–23, 2007.

[21] Y. Lv, X. Q. Wu, Y. H Zhu, X. Liang, Q. X. Cheng, and M. R Gao, "Compression behavior of basalt fiber reinforced polymer tube confined coconut fiber reinforced concrete," *Advances in Materials Science and Engineering*, vol. 2018, Article ID 7982396, 10 pages, 2018.

[22] ASTM, *Standard Test Method for Tensile Properties of Polymer Matrix Composite Materials, ASTM D3039-08*, ASTM, West Conshohocken, PA, USA, 2008.

[23] L. Yan, "Effect of alkali treatment on vibration characteristics and mechanical properties of natural fabric reinforced composites," *Journal of Reinforced Plastics and Composites*, vol. 31, no. 13, pp. 887–896, 2012.

[24] ACI 211, *Standard Test Methods for Compressive Strength of Cylindrical Concrete Specimens*, ACI, Farmington Hills, MI, USA, 2012.

[25] ASTM, *Standard Test Method for Flexural Strength of Concrete, ASTM C78-09*, ASTM, West Conshohocken, PA, USA, 2009.

[26] A. Z. Fam and S. H. Rizkalla, "Flexural behavior of concrete-filled fiber-reinforced polymer circular tubes," *Journal of Composites for Construction*, vol. 6, no. 2, pp. 123–132, 2002.

[27] CAN/CSA-S6-06, *Canadian Highway Bridge Design Code*, CSA, Mississauga, Canada, 2010.

[28] ACI 318-08, *Building Code Requirements for Structural Concrete and Commentary*, ACI, Farmington Hills, MI, USA, 2007.

[29] L. Yan and N. Chouw, "Compressive and flexural behaviour and theoretical analysis of flax fibre reinforced polymer tube encased coir fibre reinforced concrete composite," *Materials & Design (1980–2015)*, vol. 52, pp. 801–811, 2013.

[30] A. Z. Fam, *Concrete-filled fibre reinforced polymer tubes for axial and flexural structural members*, Ph.D. thesis, The University of Manitoba, Winnipeg, MB, Canada, 2000.

[31] L. B. Yan, *Design and characterization of natural flax fibre reinforced polymer tube encased coir fibre reinforced concrete composite structure*, Ph.D. thesis, The University of Auckland, Auckland, New Zealand, 2014.

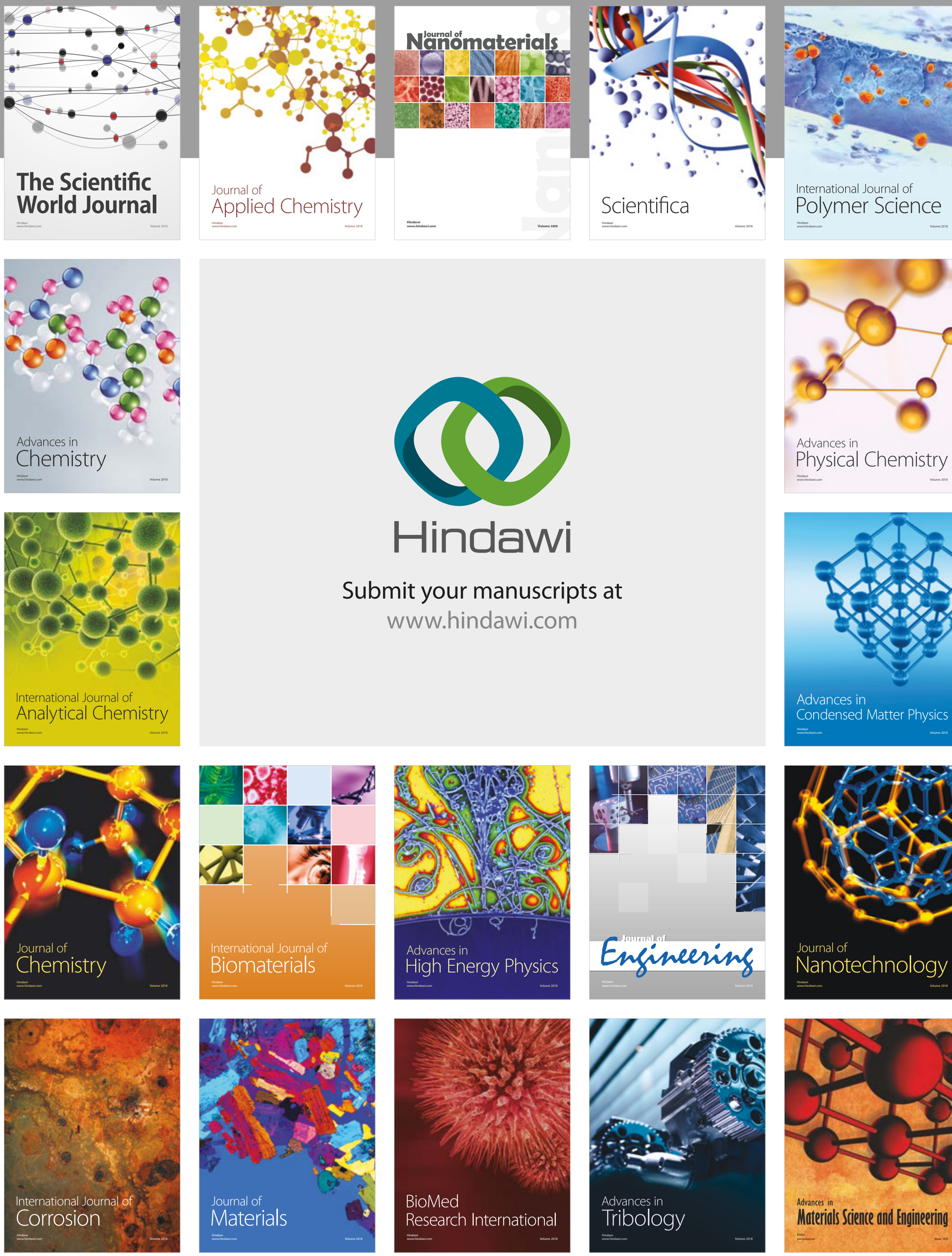
The Scientific World Journal
Journal of Applied Chemistry
Journal of Nanomaterials
Scientifica
International Journal of Polymer Science
Advances in Chemistry
Hindawi
Submit your manuscripts at
www.hindawi.com
Advances in Physical Chemistry
International Journal of Analytical Chemistry
Advances in Condensed Matter Physics
Journal of Chemistry
International Journal of Biomaterials
Advances in High Energy Physics
Journal of Engineering
Journal of Nanotechnology
International Journal of Corrosion
Journal of Materials
BioMed Research International
Advances in Tribology
Advances in Materials Science and Engineering